SAFETY AND TRANSPORT
FIRE RESEARCH

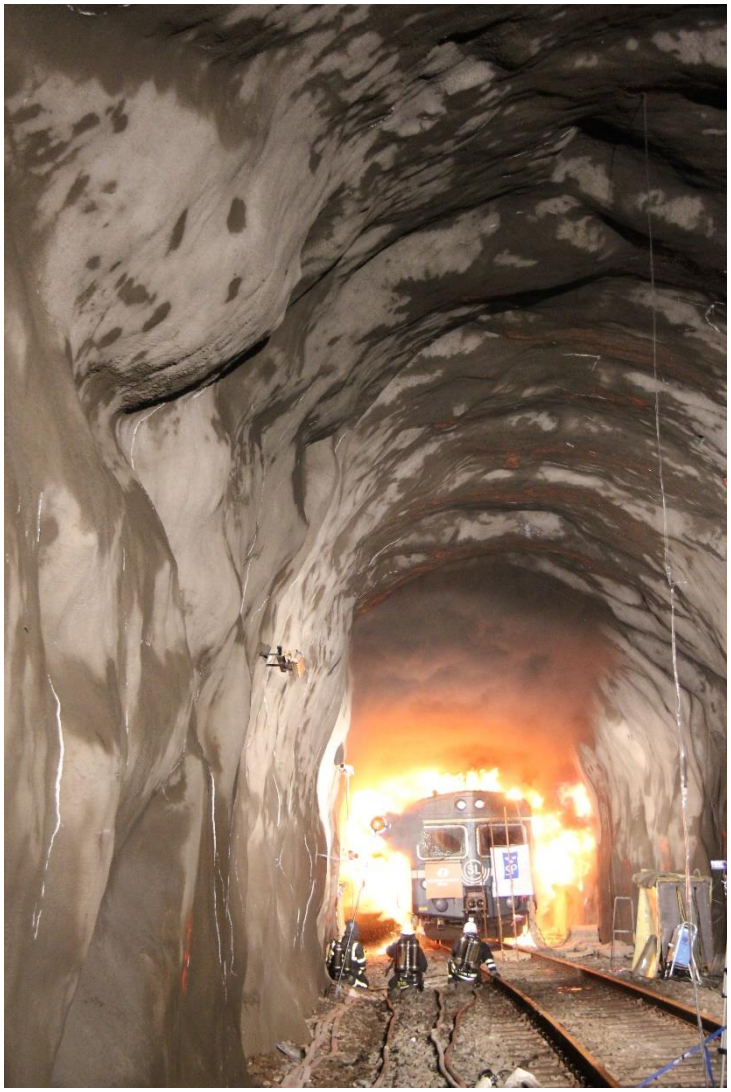

Influence of tunnel slope on smoke control

Ying Zhen Li, Haukur Ingason and Lei Jiang

RISE Report 2018:50

Influence of tunnel slope on smoke control

Ying Zhen Li, Haukur Ingason and Lei Jiang

Abstract

Influence of tunnel slope on smoke control

The critical velocity and backlayering length in sloped tunnels are investigated by numerical simulations using FDS. Simulation in two full-scale tunnels, with negative slopes ranging up to -18 % and heat release rates from 5 to 100 MW were carried out.

The results show that NFPA 502 equation [1] significantly overestimates the effect of negative slopes.

The equation proposed by Atkinson and Wu [2] is found to be in closer agreement with the results. A simplified correlation, i.e. Eq. (12), is proposed and recommended for practical use.

The previous correlation for dimensionless backlayering length, Eq. (3), is valid for tunnels of various slopes and aspect ratios, and can be used for prediction of backlayering length.

Key words: critical velocity, tunnels, sloped tunnel, FDS

RISE Research Institutes of Sweden AB

RISE Report 2018:50
ISBN: 978-91-88695-92-5
Borås

Content

Preface

The work was initiated in relation to the revision of the NFPA 502 standard [1] and the discussion on replacing existing equation to calculate the critical velocity in tunnels. The effects of the critical velocity on existing equations and different slopes of the tunnels needed further attention and exploration.

The work carried out was financed by TUSC (Tunnel Underground and Safety Center) and is a result of a discussion within a Task Group working on critical velocity which is a part of revision cycle period 2018-2019 of the NFPA 502 technical committee. The Task Group was led by Haukur Ingason who is one of the authors to this report. The authors want to thank the Task Group members on critical velocity for their efforts and co-operation during the revision process.

Summary

There have been many interesting studies carried out on the effects of slope on critical velocity. The focus of this report is on the critical velocity and backlayering length in sloping tunnels by use of numerical simulations.

Numerical simulations have been conducted using FDS in two full-scale tunnels, with negative slopes up to 18 %. A negative slope means that the fresh air is supplied at the higher elevated portal. Because of the buoyancy created by the fire, there is a need to compensate for the resistance for the longitudinal ventilation.

Good correlation between numerical simulations and some earlier work is found for critical velocity. The results show that NFPA 502 equation [1] significantly overestimates the effect of slope. Instead, equation proposed by Atkinson and Wu [2] is in closer agreement with the results. A simplified correlation, i.e. Eq. (12), is proposed and recommended for practical use.

The previous correlation for dimensionless backlayering length, Eq. (3), is valid for tunnels of various slopes and aspect ratios, and can be used for prediction of backlayering length.

1 Introduction

Smoke control is one of the key issues for any tunnel fire safety design. The two most important parameters for smoke control in tunnels with longitudinal ventilation are the critical velocity and the backlayering length.

1.1 Critical Velocity

A critical velocity is defined as the minimum longitudinal ventilation velocity to prevent reverse flow of smoke in case of fire. The dependence of critical velocity on the heat release rate (Q) in a horizontal tunnel has undergone extensive investigation. The case in an inclined tunnel has instead received less attention.

The critical velocity in a sloping tunnel, V_{cr}, can be corrected easily, based on the critical velocity in the corresponding horizontal tunnel, $V_{cr}(0)$, with the following equation:

$$V_{cr} = V_{cr}(0)K_g \tag{1}$$

The present NFPA 502 equation for sloping tunnels can be expressed as [1]:

$$K_g = 1 + 0.0374s^{0.8} \tag{2}$$

where K_g is a grade correction factor, to be applied for fires in sloping tunnels and derived from the work of Bakke & Leach [3], who studied methane layer propagation in sloping tunnels. Grant et al. [4] commented that "However, the magnitude of the density difference, and the nature of the source of the buoyant flow are very different in these two cases. It is by no means certain that gradient can be represented in such a simple manner, nor even that Bakke & Leach's data are relevant to ventilated tunnel".

Tunnel slope is defined as the ratio of uphill height to horizontal length. In other words, if the angle is θ, tunnel slope is equal to $\tan\theta$. In Eq. (2), s is the slope in %, i.e. $s = \tan\theta \times 100$. In this work, the slope is defined as positive when the entrance of fresh air is at a higher elevation than the fire source, for simplicity.

Atkinson and Wu [2] carried out a series of propane fires tests to investigate the effect of slope on critical velocity. Their equation for a slope ranging from 0° to 10° (approximately 18 %), can be simple expressed as:

$$K_g = 1 + 0.014\,\theta = 1 + 0.014\,\tan^{-1}(s/100) \tag{3}$$

Vauquelin [5] also carried out a series of tests using cold gas method to investigate the topic. Their results correlate with Atkinson et al.'s equation [2] very well. Vauquelin [5] also extended Atkinson and Wu's equation[2] to a range of -10 ° to +10 °.

Ko et al. [6] conducted experiments at five different slopes 0°, 2°, 4°, 6°, and 8° using methanol, acetone, and n-heptane and for two different fire pools. The heat release rate varied in the range 1.11 - 15.6 kW. They found that the critical velocity increases with tunnel slope for each fuel type and pool size, and that non-dimensional critical velocity could be fitted into a single correlation, regardless of the heat release rate:

$$K_g = 1 + 0.033\theta \tag{4}$$

Yi et al. [7] investigated the influence of slope in a reduced-scale model (in the range -3% ≤s≤ 3%), using methanol pool fires. They found that, as the tunnel slope increases from downhill to uphill, the critical velocity decreases at a rate that is independent of the heat release rate of the fire source, according to a fit of the form:

$$K_g = 1 + 0.034s \tag{5}$$

Chow et al. [8] studied the smoke movement in a reduced-scale tilted tunnel using gasoline 93# with three pool diameters, and for tunnel slopes up to 9°, and fitted their results by the following relation:

$$K_g = 1 + 0.022\theta \tag{6}$$

Weng et al. [9] studied the influence of the tunnel slope on the critical velocity in a reduced-scale tunnel using industrial methanol from 0 to 1%, and performed numerical simulations in two tunnels from -3% to +3%. They fitted the results based on tunnel aspect ratio φ, the ratio of tunnel width to height:

$$K_g = \begin{cases} 1 + 0.010s & \varphi \geq 1 \\ 1 + 0.024s & \varphi < 1 \end{cases} \tag{7}$$

The difference between some of these equations is shown in Figure 1. To improve the readability of the graph, only one-set of data for each experiment was plotted, together with the linear relation used by the different authors to fit their data sets. The data from Yi et al. [7] and Weng et al. [9] are not shown due to large uncertainty and the narrow range of slope. In Figure 1 it is clearly shown that the values of the grade factor K_g vary significantly from one study to another. In principle, this different behavior can be explained by the fact that these data have been obtained in different experimental set-up, with different geometrical configuration and different typologies of fire sources. The different experimental set-ups are summarized in Table 1, where we report the values of the source diameter D_i, the tunnel height H and width W, as well as their ratios, the shape of the tunnel section and the typology of fuel used.

In Appendix, the original graphs from literature are presented.

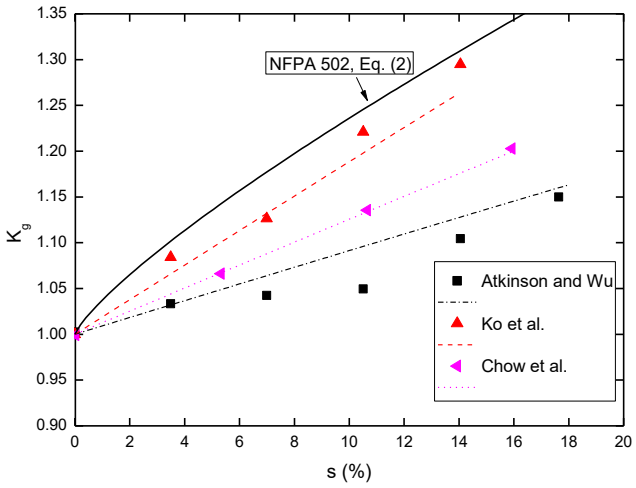

Figure 1. Grade factor K_g as a function of tunnel slope.

Table 1. Tunnel geometry of reduced scale tests in previous study.

	D_i (m)	*W/H*	D_i/W	Tunnel Shape (m)
Atkinson & Wu (propane burner)	0.10	1.12	0.36	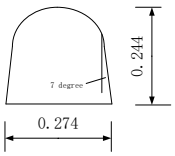
Ko et al. (pool fire)	0.065, 0.085	1	0.16, 0.21	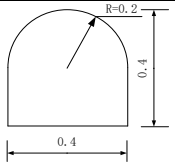
Chow et al. (pool fire)	0.16, 0.20, 0.26	1.5	0.11, 0.13, 0.17	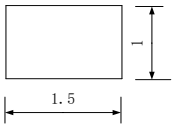

1.2 Backlayering length

The backlayering length, L_b (m), is defined as the length of the smoke backlayering upstream of the fire when the ventilation velocity is lower than the critical velocity [10]. In a longitudinally ventilated tunnel, a fresh air flow with a velocity not lower than the critical velocity at the designed heat release rate (HRR) is created to prevent smoke backlayering, which means that the tunnel is free of smoke upstream of the fire site. However, smoke stratification downstream of the fire may not persist as the ventilation velocity is too high. For this reason, a new term, “confinement velocity”, has been introduced. This is the velocity needed to prevent backlayering at a certain position, i.e. to prevent further spreading upstream. Vauquelin and Telle [11] defined the “confinement velocity” as the longitudinal velocity, as induced by the extraction ventilation system, which is necessary to prevent smoke layer development after the last exhaust vent has been activated. The reason for using such a velocity is the attempt to control backlayering and, at the same time, to preserve certain stratification.

Thomas [12] gave a simple one dimensional theoretical analysis of the backlayering length in case of a fire in a longitudinally ventilated tunnel. He correlated the backlayering length with the Froude Number. Vantelon et al. [13] carried out small-scale experiments in a 1.5 m long semicircular pipe with 0.15 m radius, and found that the ratio of backlayering length to tunnel height tended to vary as 0.3 power of a modified Richardson Number. However, in Vantelon's tests, the HRRs were very small. Further, no equation was proposed to correlate all the test data. Deberteix et al. [14] made detailed measurements of the backlayering length as well as the critical velocity in a model of the Paris metro with 0.163 m height, and related the backlayering length with a Richardson Number. However, according to their equation, the backlayering length is a negative value for a HRR of zero, which is not consistent with any physical laws.

Li et al. [15] carried out two series of tests in model scale tunnels based on a dimensional analysis, and found that the backlayering length increases with the HRR for low HRRs and is nearly

independent of HRR and dependent only on the ventilation velocity at higher HRRs. An equation for backlayering length was proposed. According to dimensional analysis and data analysis, the dimensionless backlayering length, L_b^*, was correlated with the ratio of longitudinal ventilation velocity to critical velocity [15]. It was found that the relationship between the ratio of longitudinal ventilation velocity to critical velocity and the dimensionless backlayering length, L_b^*, follows an exponential relation [15]:

$$L_b^* = \frac{L_b}{H} = 18.5 \ln(V_{cr} / V) \tag{8}$$

Where L_b is backlayering length (m) and V is longitudinal velocity.

Note that backlayering length can be estimated using the above equation in combination with an correlation for critical velocity, e.g. the one proposed in reference [16].

The above correlation was validated against data for tunnel aspect ratio of 1 and 1.15 by Li et al. [15]. Ingason and Li [17, 18] also found that the results for tunnel aspect ratio of 1.5 and 2 closely follow the same correlation.

1.3 A short summary

There have been many correlations proposed to account for the effect of slope on critical velocity and some of them vary significantly. This slope effect needs to be further investigated.

Further, the effect of slope on backlayering length will be studied and the influence of tunnel aspect ratio will also be further verified.

2 Numerical simulations

Full-scale simulations were conducted in two tunnels using FDS 6.2 [19]. The first tunnel (tunnel A) was 100 m long (L), 5 m wide (W) and 5 m high (H); the second tunnel (tunnel B) was 100 m long, 10 m wide and 5 m high. The aspect ratio (AR=W/H) is 1 for tunnel A and 2 for tunnel B. The tunnel inclination was adapted by varying gravity components in x and z direction. The tunnel walls were 0.3 m concrete. At the inlet, a ventilation velocity was fixed and at the outlet it was set 'open'. A fire source of 2 m×2 m was set to the center of the tunnel, making both the downstream section and upstream section 50 m. The heat release rates simulated were 5 MW, 10 MW, 20 MW, 50 MW and 100 MW. The grid size was 0.2 m, referring to the literature [10]. A set of thermocouples were set 0.03 m below the ceiling, from 30 m to 60 m with an interval of 0.5 m. The simulation time was 600 s. The location of the backlayering was determined when the temperature was 5 ℃ higher than the ambient. The simulation cases for tunnel A are listed in Table 2. In tunnel B, the slopes were varied only at 0, 2° and 6°. In total, there were 36 cases simulated.

The numerical results in the horizontal tunnel is obtained first and then compared with a correlation proposed by Li and Ingason [16]:

$$V_{cr}^{*} = \frac{V_{cr}}{\sqrt{gH}} = \begin{cases} 0.81\varphi^{-1/12}Q^{*1/3} & Q^{*} \le 0.15\varphi^{1/4} \\ 0.43 & Q^{*} > 0.15\varphi^{1/4} \end{cases} \quad (9)$$

where $Q^{*} = \frac{Q}{\rho_0 C_p T_0 g^{1/2} H^{5/2}}$, $\varphi = \frac{W}{H}$, C_p is specific heat capacity, ρ_0 and T_0 are the ambient air density and temperature, respectively, g is gravity acceleration.

Table 2. Simulation cases for tunnel A, x under calculation.

s (%) / Q (MW)	0	3.5	7.0	10.5	14.0	17.6
5	√	√	√	√	√	√
10	√	√		√		
20	√	√	√	√	√	√
50	√	√		√		
100	√	√		√		

Figure 2 shows the comparison of the numerical results in the horizontal tunnel and the correlation Eq. (9). Good agreement is found between the numerical data and the correlation, which indicates the validity of current numerical set up. When slope changes, the critical velocity becomes larger and a correction is needed, as suggested in the Introduction.

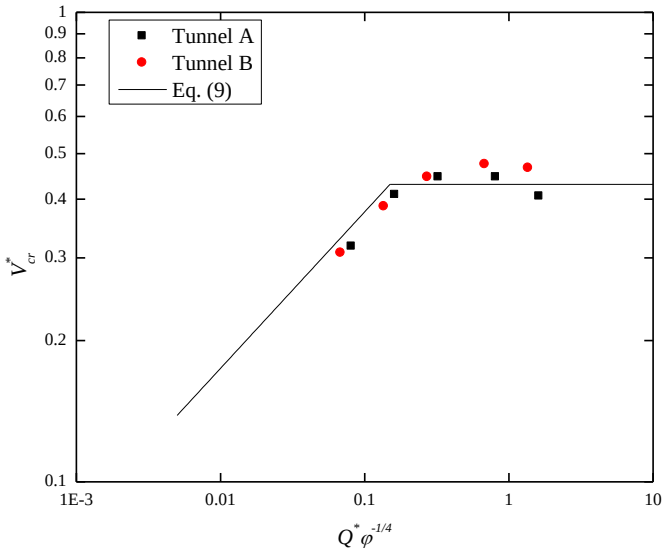

Figure 2. Numerical results in the horizontal tunnel, compared with Eq. (9).

3 Results

In the following, results for critical velocity and backlayering lengths are analyzed and compared with previous models.

3.1 Influence of slope on critical velocity

3.1.1 Comparison with existing correlations

The numerical results of grade factor K_g as a function of tunnel slope is shown in Figure 3, together with Eq. (2) and Eq. (3). Our results suggest that Eq. (3) is suitable to account the influence of tunnel slope on the critical velocity, while Eq. (2) significantly overestimates the effect of the slope.

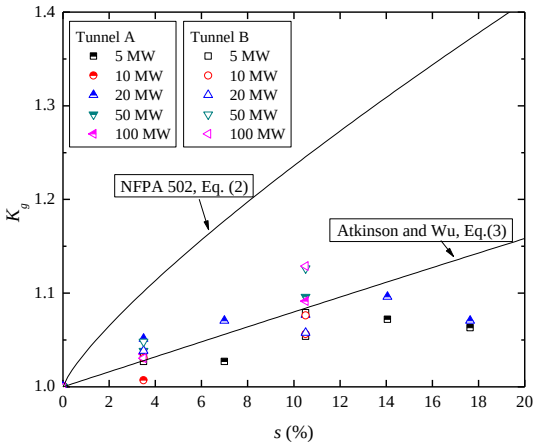

Figure 3. Numerical results of grade factor Kg as a function of tunnel slope (in percentage), compared with Eq. (2) and Eq. (3).

The influence of slope on the movement of smoke is mainly related to the 'stack effect', i.e. to the role of the component of buoyancy along the tunnel axis. It is suggested in [10] that a wider tunnel indicates a thinner smoke layer and smaller buoyancy force, thus a smaller Kg, which is in an agreement with Eq. (7). However, this influence of tunnel width is not obvious in current study with AR=1 and AR=2.

Using Eq. (9) for the critical velocity in horizontal tunnels, the critical velocity in sloping tunnels is then expressed as:

$$V_{cr}^{*} = \frac{V_{cr}}{\sqrt{gH}} = \begin{cases} 0.81(1 + 0.014\tan^{-1}(s/100))\varphi^{-1/12}Q^{*1/3} & Q^{*} \le 0.15\varphi^{1/4} \\ 0.43\ \ (1 + 0.014\tan^{-1}(s/100)\ ) & Q^{*} > 0.15\varphi^{1/4} \end{cases} \quad (10)$$

All the numerical data in Figure 3 are then reorganized and compared with Eq. (10) in Figure 4.

In the above equation, the angle obtained by $\tan^{-1}$ should be in radian, noting that one radian is about $180/\pi$ (about 57.3 °).

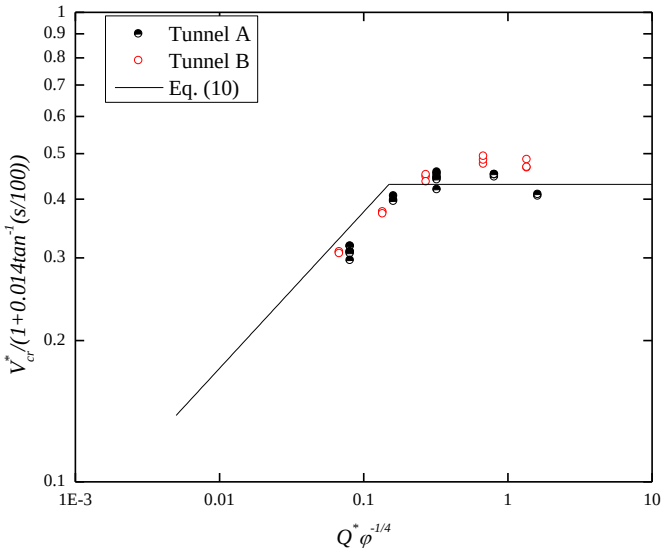

Figure 4. Numerical results of $V_{cr}^*/(1+0.014\tan^{-1}(s/100))$ as a function of $Q^*\varphi^{-1/4}$, compared with Eq. (10).

3.1.2 Simplifications for practical use

Note that in the above analysis, the inverse function atan corresponds to angle in degree. However, in most applications, radians are obtained while using such functions in program, e.g. Excel sheet. Noting that 0.014×57.3 ≈ 0.80, the above correlation could be revised as follows:

$$V_{cr}^* = \frac{V_{cr}}{\sqrt{gH}} = \begin{cases} 0.81(1+0.8\tan^{-1}(s/100))\varphi^{-1/12}Q^{*1/3} & Q^* \le 0.15\varphi^{1/4} \\ 0.43(1+0.8\tan^{-1}(s/100)) & Q^* > 0.15\varphi^{1/4} \end{cases} \quad (11)$$

The above equation can be further simplified, noting that for a slope, *s*, in the range of -30 and 30, we have:

$$s/100 \approx \tan^{-1}(s/100) \quad (12)$$

A comparison of $\tan^{-1}(s/100)$ and s/100 as a function of slope is shown in Figure 7. The difference increases with the absolute value of slope, s, but the error is only around 0.3 % for a slope of 10 % (s=10) and 2.9 % for a slope of 30 % (s=30). Even for a slope of 60 % (s=60), the difference is around 11 %. Further, for a negative slope (downhill), the value for s/100 is always slightly greater than $\tan^{-1}(s/100)$, indicating use of Eq. (9) produces slightly conservative results.

By use of Eq. (12), Eq. (3) can be simplified as follows:

$$K_g = 1 + 0.008s \quad (13)$$

To verify the use of Eq. (13), the results shown in Figure 3 are replotted in Figure 6. The red line corresponds to Eq. (13) and the black line to Eq. (3). Clearly, it shows in Figure 6 that the

difference in the grade correction factor, Kg, caused by the use of Eq. (12) is much smaller than the difference between $\tan^{-1}(s/100)$ and s/100 discussed above. The difference is only about 0.025 % for a slope of 10 % (s=10) and 0.55 % for a slope of 30 % (s=30). In other words, the difference is negligible in practical use.

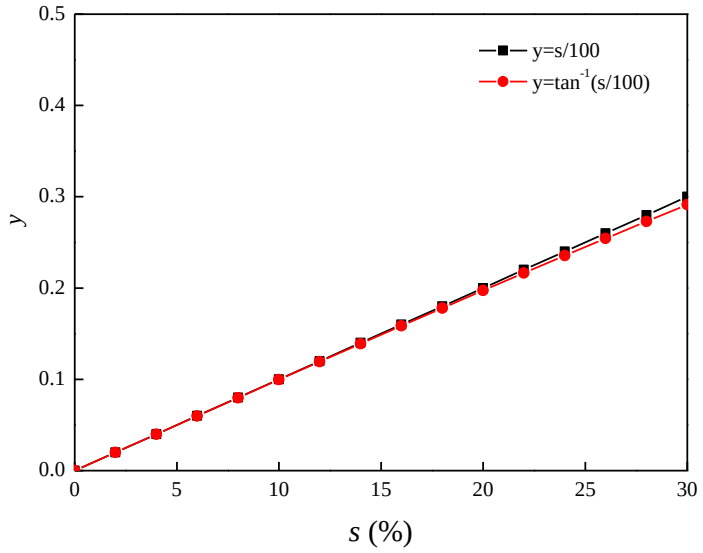

Figure 5. Comparison of $\tan^{-1}(s/100)$ and s/100 as a function of slope.

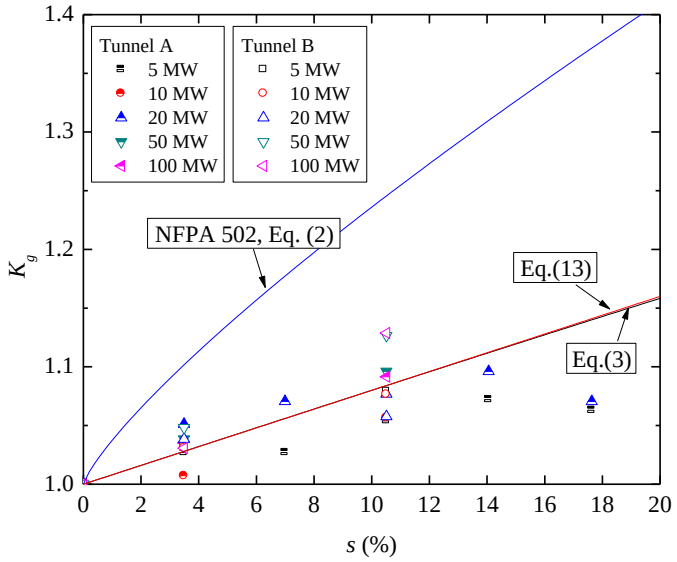

Figure 6. Numerical results of grade factor Kg as a function of tunnel slope (in percentage), compared with Eq. (2), Eq. (3) and Eq. (13).

By use of Eq. (13), Eq. (11) can, therefore, be written as follows:

$$V_{cr}^{*} = \frac{V_{cr}}{\sqrt{gH}} = \begin{cases} 0.81(1 + 0.008\,s)\varphi^{-1/12}Q^{*1/3} & Q^{*} \le 0.15\varphi^{1/4} \\ 0.43(1 + 0.008\,s\,) & Q^{*} > 0.15\varphi^{1/4} \end{cases} \quad (14)$$

3.2 Influence of slope on backlayering length

Figure 7 and Figure 8 show the dimensionless backlayering lengths for various slopes and HRRs as a function of the ratio of longitudinal velocity to critical velocity for AR=1 and AR=2, respectively. Predictions by Eq. (8) are also shown for comparison.

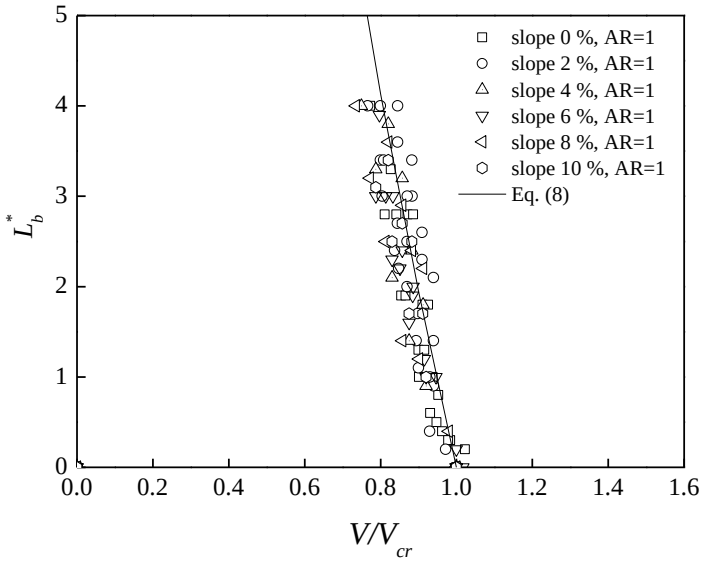

Figure 7. Dimensionless backlayering length as a function of the ratio of longitudinal velocity to critical velocity for various slopes and HRRs (AR=1).

It is shown in Figure 7 and Figure 8 that all the data comply with Eq. (8) well. These data refer to tunnels of various slopes and tunnel aspect ratios and different HRRs. Recalling the previous validation against data for tunnel aspect ratio of 1 - 1.15 [15] and 1.5 – 2 [17, 18] discussed in Section 1.2, the good agreement indicates that Eq. (8) is applicable to predict backlayering length for tunnels of various slopes and tunnel aspect ratios and different HRRs.

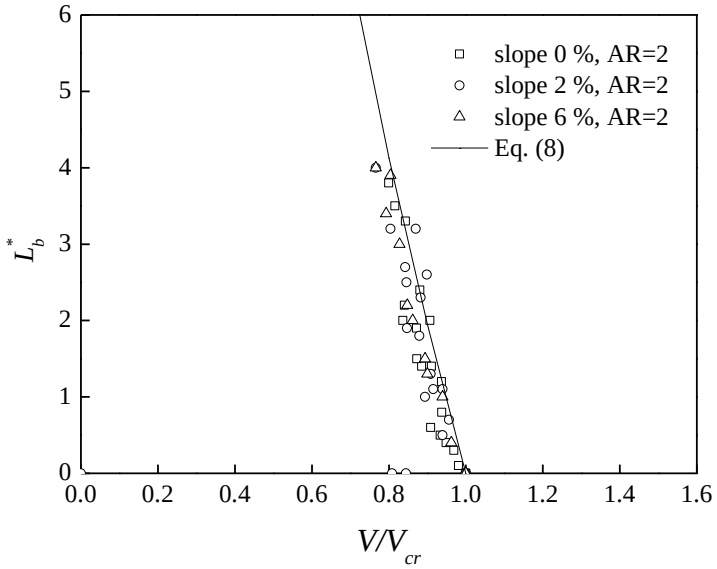

Figure 8. Dimensionless backlayering length as a function of the ratio of longitudinal velocity to critical velocity for various slopes and HRRs (AR=2).

4 Conclusions

In this report the critical velocity and backlayering length in sloping tunnels is investigated. Numerical simulations have been conducted in two full scale tunnels, with slopes up to 18 %. The results show that NFPA 502 equation [1] significantly overestimates the effect of slope on critical velocity. Instead, Eq. (3) proposed by Atkinson and Wu [2] is in closer agreement with the results. A simplified correlation, i.e. Eq. (14), is proposed and recommended for practical use. Further, the previous correlation for dimensionless backlayering length, Eq. (3), is valid for tunnels of various slopes and aspect ratios, and can be used for prediction of backlayering length.

After considering the slope effect, the equation proposed for critical velocity is:

$$V_{cr}^{*} = \frac{V_{cr}}{\sqrt{gH}} = \begin{cases} 0.81(1 + 0.008\,s)\varphi^{-1/12}Q^{*1/3} & Q^{*} \le 0.15\varphi^{1/4} \\ 0.43(1 + 0.008\,s\,) & Q^{*} > 0.15\varphi^{1/4} \end{cases} \quad (14)$$

where $Q^{*} = \frac{Q}{\rho_0 C_p T_0 g^{1/2} H^{5/2}}$, $\varphi = \frac{W}{H}$, W is tunnel width (largest width for an arcuate tunnel), H is tunnel height, C_p is specific heat capacity, ρ_0 and T_0 are the ambient air density and temperature, respectively, g is gravity acceleration, s is slope (%).

The backlayering length can be calculated based on the ratio of longitudinal velocity to the critical velocity using the following correlation:

$$L_b^{*} = \frac{L_b}{H} = 18.5\ln(V_{cr}/V) \quad (8)$$

where V is longitudinal velocity. The above equation has been found to be applicable for various tunnel slopes and aspect ratios.

Note that in this work, the slope is defined as positive when the entrance of fresh air is at a higher elevation than the fire source, for simplicity.

References

1. *NFPA 502 - Standard for Road Tunnels, Bridges, and Other Limited Access Highways*. 2017 Edition, National Fire Protection Association.
2. Atkinson, G.T. and Y. Wu, *Smoke Control in Sloping Tunnels.* Fire Safety Journal, 1996. **27**: p. 335-341.
3. Bakke P. and Leach S. J., *Turbulent diffusion of a buoyant layer at a wall.* Appl. Sci. Res., 1965. **15**: p. 97-136.
4. Grant, G.B., S.F. Jagger, and C.J. Lea, *Fires in tunnels.* Phil. Trans. R. Soc. Lond., 1998. **356**: p. 2873-2906.
5. Vauquelin O., *Parametrical study of the back flow occurrence in case of a buoyant release* Experimental Thermal and Fluid Science, 2005. **29**: p. 725-731.
6. Ko, G.H., S.R. Kim, and H.S. Ryou, *An experimental study on the effect of slope on the critical* Journal of Fire Sciences, 2010. **28**: p. 27–47.
7. Yi L., et al., *An experimental study on critical velocity in sloping tunnel with longitudinal ventilation under fire.* Tunnelling and Underground Space Technology, 2014. **43**: p. 198-203.
8. Chow W.K., et al., *Smoke movement in tilted tunnel fires with longitudinal ventilation.* Fire Safety Journal, 2015. **75**: p. 14–22.
9. Weng M.C., et al., *Study on the critical velocity in a sloping tunnel fire under longitudinal ventilation.* Applied Thermal Engineering, 2016. **94**: p. 422–434.
10. Li, Y.Z. and H. Ingason, *Overview of research on fire safety in underground road and railway tunnels.* Tunnelling and Underground Space Technology, 2018. **81**: p. 568-589.
11. Vauquelin, O. and D. Telle, *Definition and experimental evaluation of the smoke "confinement velocity" in tunnel fires*. Fire Safety Journal, 2005. **40**: p. 320-330.
12. Thomas, P., *The movement of buoyant fluid against a stream and the venting of underground fires*. 1958, Fire Research Station: Boreham Wood.
13. Vantelon, J.P., et al. *Investigation of Fire-Induced Smoke Movement in Tunnels and Stations: An Application to the Paris Metro*. in *IAFSS Fire Safety Science-Proceedings of the third international symposium*. 1991. Edinburg.
14. Deberteix P., Gabay D., and Blay D. *Experimental study of fire-induced smoke propagation in a tunnel in the presence of longitudinal ventilation*. in *Proceedings of the International Conference on Tunnel Fires and Escape from Tunnels*. 2001. Washington.
15. Li, Y.Z., B. Lei, and H. Ingason, *Study of critical velocity and backlayering length in longitudinally ventilated tunnel fires.* Fire Safety Journal, 2010. **45**: p. 361-370.
16. Li, Y.Z. and H. Ingason, *Effect of cross section on critical velocity in longitudinally ventilated tunnel fires.* Fire Safety Journal, 2017. **91**: p. 303–311.
17. Ingason, H. and Y.Z. Li, *Model scale tunnel fire tests with point extraction ventilation*. Journal of Fire Protection Engineering, 2011. **21**(1): p. 5-36.
18. Ingason, H. and Y.Z. Li, *Model scale tunnel fire tests with longitudinal ventilation*. Fire Safety Journal, 2010. **45**: p. 371-384.
19. McGrattan, K., et al., *Fire Dynamics Simulator User's Guide (Version 6)* 2015, National Institute of Standards and Technology: USA.

Appendix

Equation (3)

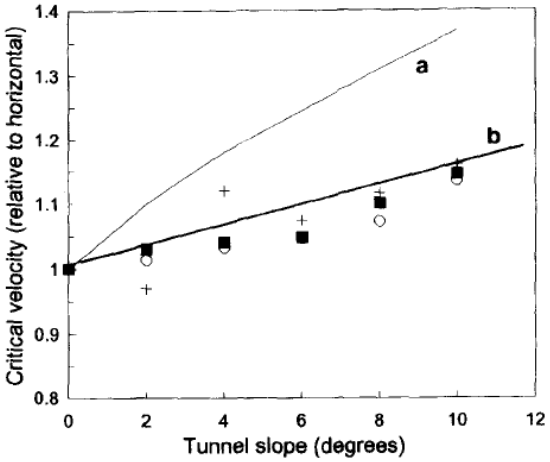

Figure 9. Critical velocity vs. tunnel slope (From Atkinson & Wu [4]). a is Eq. (2) and b is the proposed equation Eq. (3).

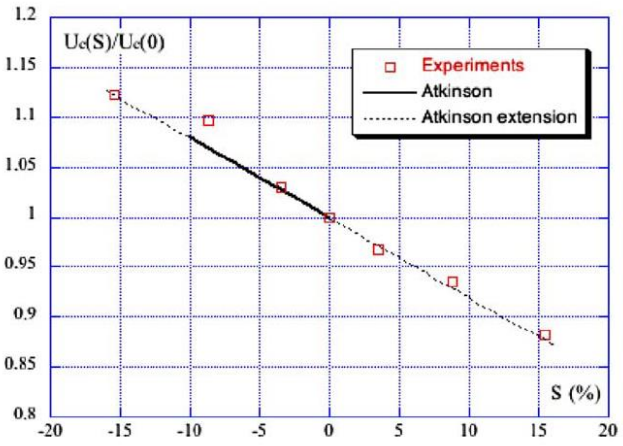

Fig. 5. Critical velocity as a function of the channel slope.

Figure 10. Critical velocity vs. tunnel slope (From Vauquelin [5]).

Equation (4)

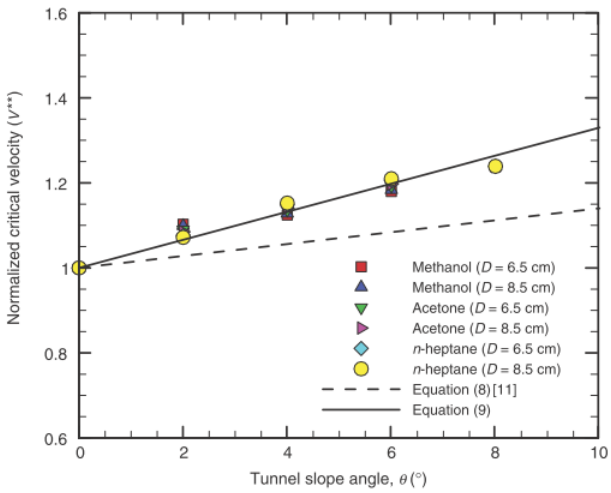

Figure 11. Critical velocity vs. tunnel slope (From Ko et.al [6]). Eq. (8) is the proposed equation Eq. (3), Eq. (9) is the linear fit Eq. (4).

Equation (5)

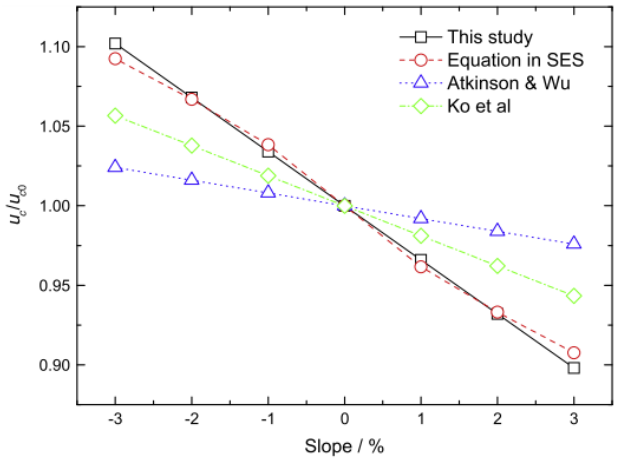

Figure 12. Critical velocity vs. tunnel slope (From Yi et.al [7]).

Equation (6)

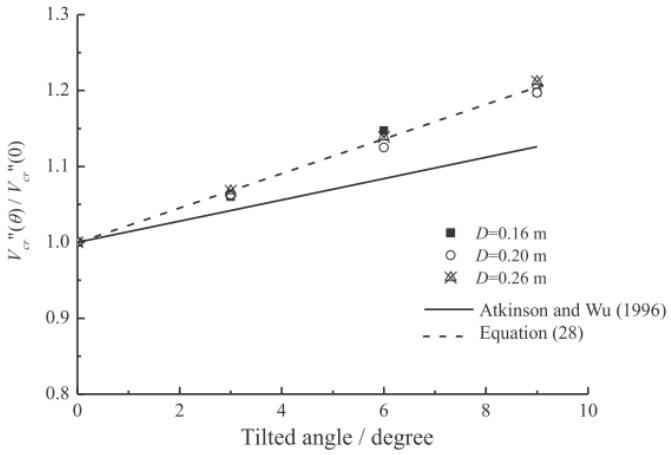

Figure 13. Critical velocity vs. tunnel slope (From Chow et.al [8]). Eq. (28) is the linear fit Eq. (6).

Equation (7)

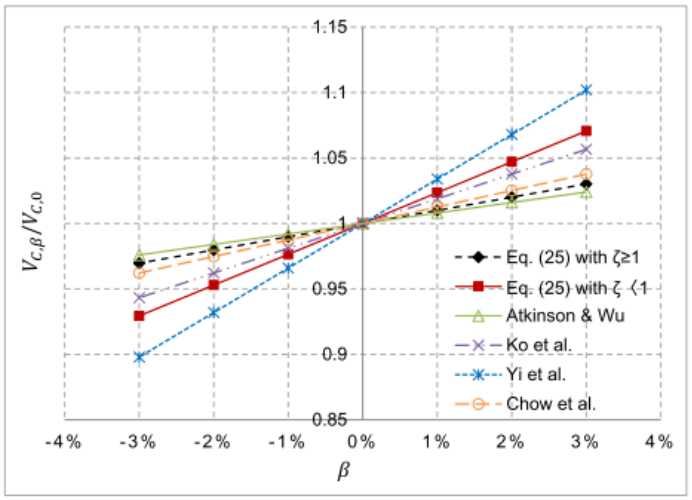

Fig. 11. Comparison of the variation of $V_{c,\beta}/V_{c,0}$ with tunnel slope β by different models.

Figure 14. Critical velocity vs. tunnel slope (From Weng et.al [9]). Eq. (25) is the linear fit Eq. (7).

Through our international collaboration programmes with academia, industry, and the public sector, we ensure the competitiveness of the Swedish business community on an international level and contribute to a sustainable society. Our 2,200 employees support and promote all manner of innovative processes, and our roughly 100 testbeds and demonstration facilities are instrumental in developing the future-proofing of products, technologies, and services. RISE Research Institutes of Sweden is fully owned by the Swedish state.

I internationell samverkan med akademi, näringsliv och offentlig sektor bidrar vi till ett konkurrenskraftigt näringsliv och ett hållbart samhälle. RISE 2 200 medarbetare driver och stöder alla typer av innovationsprocesser. Vi erbjuder ett 100-tal test- och demonstrationsmiljöer för framtidssäkra produkter, tekniker och tjänster. RISE Research Institutes of Sweden ägs av svenska staten.

RISE Research Institutes of Sweden AB
Box 857, 501 15 BORÅS
Telefon: 010-516 50 00
E-post: info@ri.se, Internet: www.ri.se

Fire REsearch
RISE Report 2018:50
ISBN: